LA-UR-17-20437 (Accepted Manuscript)

Magnetic resonance force microscopy with a paramagnetic probe

Berman, Gennady Petrovich
Gorskov, V.N.
Tsifrinovich, V.I.

To be published in: Physics Letters A

DOI to publisher's version: 10.1016/j.physleta.2017.02.026

Accepted Manuscript

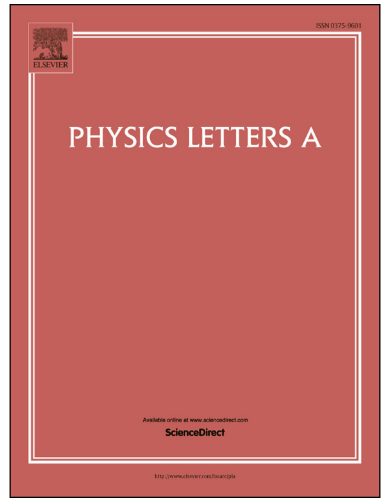

Magnetic resonance force microscopy with a paramagnetic probe

G.P. Berman, V.N. Gorshkov, V.I. Tsifrinovich

PII: S0375-9601(17)30184-6
DOI: http://dx.doi.org/10.1016/j.physleta.2017.02.026
Reference: PLA 24361

To appear in: *Physics Letters A*

Received date: 25 January 2017
Revised date: 14 February 2017
Accepted date: 20 February 2017

Highlights

- We consider extension of magnetic resonance force microscopy replacing a ferromagnetic probe with a paramagnetic one.
- We analyze the dynamics of the interacting magnetic moments on a probe and a sample.
- We have found a proper sequence of electromagnetic pulses which provide a significant deflection of the cantilever.

Magnetic Resonance Force Microscopy with a Paramagnetic Probe

G.P. Berman[1], V.N. Gorshkov[2], and V.I. Tsifrinovich[3]

[1] *Bioscience Division, B-11, Los Alamos National Laboratory and the New Mexico Consortium, Los* Alamos, NM, 87544, USA
[2] *National Technical University of Ukraine, "Igor Sikorsky Kyiv Polytechnic Institute", Ukraine*
[3] *Department of Applied Physics, NYU Tandon School of Engineering, Brooklyn, NY 11201, USA*

Abstract

We consider theoretically extension of magnetic resonance force microscopy (MRFM) replacing a ferromagnetic probe on a cantilever tip (CT) with a paramagnetic one (PMRFM). The dynamics of the interaction between the paramagnetic probe and a local magnetic moment in a sample is analyzed, using a quasi-classical approach. We show that the application of a proper sequence of electromagnetic pulses provides a significant deflection of the CT from the initial equilibrium position. Periodic application of these sequences of pulses results in quasi-periodic CT deflections from the equilibrium, which can be used for detection of the magnetic moment in a sample.

PACS numbers: 76.30.-v; 05.40.-a; 07.55.-w

I. INTRODUCTION

Our work was inspired by spectacular achievements in magnetic resonance force microscopy (MRFM) [1,2] culminating in a single spin detection [3] and a nanometer scale resolution [4]. We consider extension of MRFM to a situation when a ferromagnetic particle on a cantilever tip (CT) is replaced by a paramagnetic one (PMRFM). The magnetic moment of the ferromagnetic particle in MRFM remains constant: its magnitude and direction do not change. In contrary, the magnetic moment of the paramagnetic particle is a dynamical variable which should be found from the equations of motion. We consider a dynamical detection scheme using a quasi-classical theory.

The main idea of our model is the following. A paramagnetic particle placed on the CT interacts with a local magnetic moment in a sample via the dipole-dipole interaction. Due to this interaction the CT is shifted from its equilibrium position. We will describe the direction of the magnetic moments (or just "moments"). Initially both moments are oriented in the direction of the strong external magnetic field (the up-direction). Using a special "trained" sequence of resonant radiofrequency (*rf*) pulses, one quickly deflects the moments from the up-direction. We consider a critically damped cantilever with a paramagnetic particle which promptly changes its equilibrium position following the change of the magnetic force. After this, both magnetic moments and the CT slowly return to their equilibrium positions in the process of the spin-lattice relaxation. Our

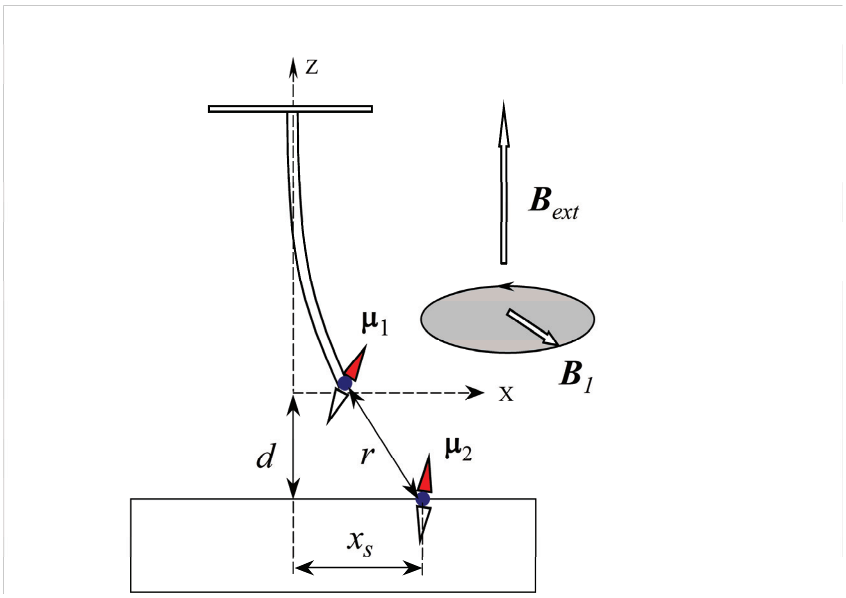

FIG. 1: The geometry of the PMRFM. $\vec{\mu}_1$ and $\vec{\mu}_2$ are the magnetic moments on the CT and in the sample, $\vec{B}_{ext}$ and $\vec{B}_1$ are the permanent and rotating magnetic fields applied to the magnetic moments. The origin is placed in the equilibrium position of the CT with no paramagnetic particle. The coordinates of $\vec{\mu}_2$ are $(x_s, 0, -d)$.

protocol consists of a periodic application of the trained sequence of rf pulses which results in quasi-periodic dynamics of the CT. This dynamics can be used for detection of the local magnetic moment in a sample.

II. EQUATIONS OF MOTION AND PARAMETERS

The geometry of the suggested set-up is shown in Fig. 1. The Hamiltonian of the system can be written as,

$$H = \frac{p_x^2}{2m_c} + \frac{1}{2}k_c x_c^2 - \left(\vec{B}_{ext} + \vec{B}\right)\left(\vec{\mu}_1 + \vec{\mu}_2\right) + \frac{\mu_0}{4\pi}\frac{3\left(\vec{\mu}_1 \cdot \vec{n}\right)\left(\vec{\mu}_2 \cdot \vec{n}\right) - \vec{\mu}_1 \cdot \vec{\mu}_2}{r^3}, \tag{1}$$

where p_x and x_c are the momentum and the coordinate of the CT, m_c and k_c are the effective mass and the spring constant of the CT, $\vec{n}(x_c)$ is the unit vector which points from $\vec{\mu}_1$ to $\vec{\mu}_2$, $x_- = x_s - x_c$, $r = \left(x_-^2 + d^2\right)^{\frac{1}{2}}$, x_s and $(-d)$ are the x- and z-coordinates of $\vec{\mu}_2$. $\vec{B}_{ext}$ is the permanent magnetic field oriented in the positive z-direction, $\vec{B}_1$ is the transversal magnetic field rotating with the frequency $\omega = \gamma B_{ext}$, where γ is the magnitude of the electron gyromagnetic ratio.

If both magnetic moments point in the positive z-direction, the equilibrium position of the CT, $x_c = x_0$, can be found from the equation, $\partial H / \partial x_c = 0$, or

$$x_c = f\left(x_c\right), \quad f\left(x_c\right) = \frac{3\mu_0\mu_1\mu_2}{4\pi k_c}\frac{\left(x_-/r\right)\left(5d^2/r^2 - 1\right)}{r^4}. \tag{2}$$

Below we use the dimensionless quantities: we take the Bohr's magneton, μ, being the unit of the magnetic moment, the equilibrium position, x_0, being the unit of length, the frequency of the CT, $\omega_c = \left(k_c / m_c\right)^{1/2}$, being the unit of the angular frequency, and $1/\omega_c$ being the unit of time. In this notation, the equations of motion for the dimensionless quantities, $\vec{\mu}_1$, $\vec{\mu}_2$, and x_c, in the rotating frame are,

$$\begin{aligned}
&\dot{\vec{\mu}}_1 = \vec{\Omega}_1 \times \vec{\mu}_1 - \left(\vec{\mu}_1 - \vec{\mu}_1^*\right)/\tau_s, \\
&\dot{\vec{\mu}}_2 = \vec{\Omega}_2 \times \vec{\mu}_2 - \left(\vec{\mu}_2 - \vec{\mu}_2^*\right)/\tau_s, \\
&\ddot{x}_c + x_c + \dot{x}_c / Q = \mu_{1z}\mu_{2z} f'\left(x_c\right), \\
&\vec{\Omega}_1 = \left(\omega_R - R\mu_{2x}, -R\mu_{2y}, \omega_d\mu_{2z}\right), \\
&\vec{\Omega}_2 = \left(\omega_R - R\mu_{1x}, -R\mu_{1y}, \omega_d\mu_{1z}\right), \\
&R = \frac{\gamma\mu_0\mu}{8\pi\omega_c x_0^3}\frac{1}{r^3}, \\
&\omega_d = 2R\left(3d^2/r^2 - 1\right), \ \omega_R = \gamma B_1 / \omega_c, \\
&f'\left(x_c\right) = \frac{3\mu_0\mu^2}{4\pi k_c x_0}\frac{\left(x_-/r\right)\left(5d^2/r^2 - 1\right)}{r^4}.
\end{aligned} \tag{3}$$

Here, $\vec{\mu}_{1,2}^*$, denote vectors $\vec{\mu}_{1,2}$ in the equilibrium, τ_s is the spin relaxation time, Q is the cantilever quality factor, R and ω_d are associated with the dipole field, ω_R is the Rabi frequency. (All quantities in Eqs. (3) are dimensionless.) In Eqs. (3), we ignored the contribution of quickly oscillating transversal components of $\vec{\mu}_{1,2}$ into the force acting on the cantilever. Thus, this force depends on the product, $\mu_{1z}\mu_{2z}$. Also, we took into consideration only a resonant rotating component of the transversal dipole field.

For numerical simulations we assume the following parameters. The cantilever spring constant, $k_c = 1\mu N / m$, the cantilever frequency, $\omega_c / 2\pi = 10kHz$, $B_1 = 300\mu T$, $x_s = 600pm$, $d = 400pm$, $\tau_s \approx 79.6\mu s$. For these values of parameters, the equilibrium displacement of the CT is, $x_0 \approx 540pm$. At the temperature below $T_* = 20mK$, the mechanical noise,

$$x_{rms} = \sqrt{k_B T / k_c}\ , \tag{4}$$

will be smaller than the equilibrium displacement, x_0.

We consider a critically damped cantilever with $Q = 0.5$ to insure the fast return of the CT to the equilibrium position. (The corresponding CT time constant is, $\tau_c = 2Q / \omega_c = 16\mu s$.) The dipole field in our geometry is,

$$B_d \sim 2\mu_0\mu / 4\pi d^3 \approx 30mT.$$

We assume that the external magnetic field, B_{ext}, is much greater than B_d. Also, we assume that $2\mu B_{ext} >> k_B T$, so the magnetic moments point initially in the positive z-direction. The dimensionless values of our parameters are,

$$d \approx 0.74.\ x_s \approx 1.11,\ \omega_R = 840,\ \tau_s = 5,\ \tau_c = 1.$$

We take the ultimate values of the magnetic moments,

$$\mu_1^* = \mu_2^* = \mu\ .$$

III. THE DYNAMICAL REGIME OF THE PMRFM

Our purpose is to find a predictable quasi-periodic motion of the CT with maximum possible deviation from the equilibrium. Our strategy is the following. We apply rf pulses to provide a maximum possible change of the magnetic force between two magnetic moments. A critically damped CT quickly moves to the new equilibrium position. After this, two spins and the CT return to their initial state, and the sequence of pulses can be repeated.

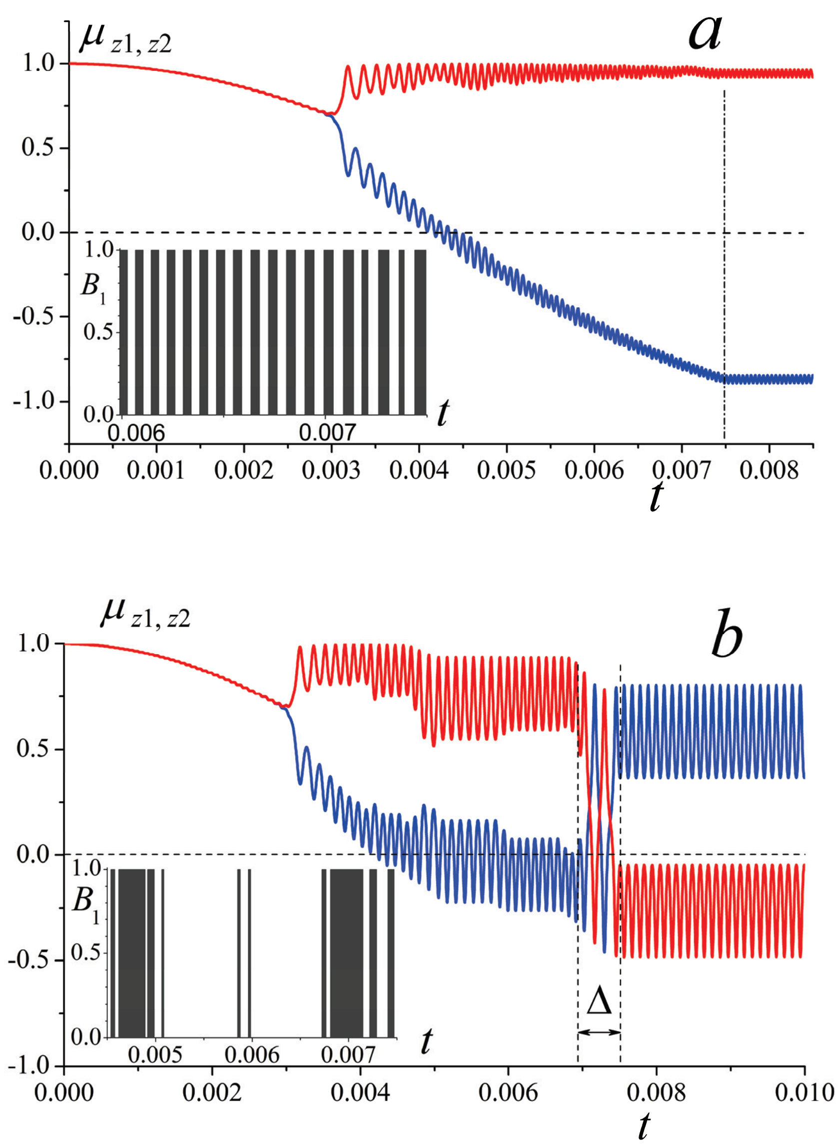

FIG. 2: The dynamics of the z-components of magnetic moments; (a): the sequence of pulses conditioned on the direction of the magnetic moment on the CT, $\vec{\mu}_1$ (b): the same for the magnetic moment in the sample, $\vec{\mu}_2$. Insert shows the sequence of pulses. The pulses are applied during the time interval, $0 \le t \le 7.5 \times 10^{-3}$. Vertical dashed lines indicate the end of action of the rf pulses. In the time interval, Δ, shown in (b), the period of oscillations of $\vec{\mu}_1$ and $\vec{\mu}_2$ doubles.

To provide the maximum change of the magnetic force, we apply the *rf* pulses along the x-axis of the rotating frame when the y-component of one of the magnetic moments is negative. In this case, the z-component of the corresponding magnetic moment decreases, i.e. the magnetic moment deflects from the initial (+z) direction. So, the pulses are conditioned on the direction of one of the moments. Fig. 2a, demonstrates the change of the z-component of two magnetic moments when we control the y-component of $\vec{\mu}_1$ (which is placed on the CT). During the time-interval, 7.5×10^{-3}, we apply 183 *rf* pulses. The sequence of pulses is rather regular. (See insert in Fig. 2a.) One can see that initially $\vec{\mu}_1$ and $\vec{\mu}_2$ move together, but after some time the deflection of $\vec{\mu}_1$ from the positive z -direction continues, while $\vec{\mu}_2$ returns to the initial direction.

Fig. 2b, demonstrates a similar but more irregular dynamics when we control the *y*- component of $\vec{\mu}_2$ (which is placed in the sample). During the same time interval, 7.5×10^{-3}, we apply 130 *rf* pulses; the sequence of pulses is rather irregular. (See insert in Fig. 2b.) Note, that during the time-interval Δ (see fig. 2b), we detected a doubling of the oscillation period for the z-components of $\vec{\mu}_1$ and $\vec{\mu}_2$. After the action of the pulse sequence, the z -components of $\vec{\mu}_1$ and $\vec{\mu}_2$ in Fig. 2a oscillate in antiphase providing the conservation of the magnetic energy.

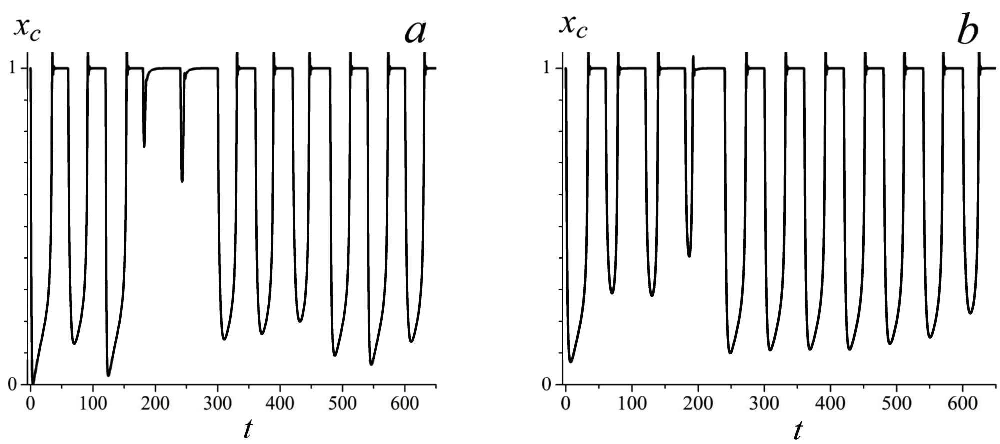

FIG. 3: The dynamics of the CT under the periodic application of the pulse sequences; (a): for pulse sequences shown in Fig. 2a; (b): for pulse sequences shown in Fig. 2b. The repetition period of pulse sequences is, $T = 60$.

In order to avoid confusion we should note that in the numerical experiments we control the y-component of a magnetic moment in order to choose the optimal sequence of the *rf* pulses. In the suggested experiment one does not have to control the direction of the magnetic moment. Instead one should use the sequences of pulses, suggested in this paper, which will provide the maximum deviation of the CT from the equilibrium position.

The most striking peculiarity of the magnetic moments and the cantilever dynamics is the following. When we apply the same sequence of pulses, we cannot reproduce the pictures shown in Fig. 2. The tiny "numerical noise", which is always present in computer simulations, causes a significant change in the dynamics. This situation is typical for nonlinear systems in the regime of

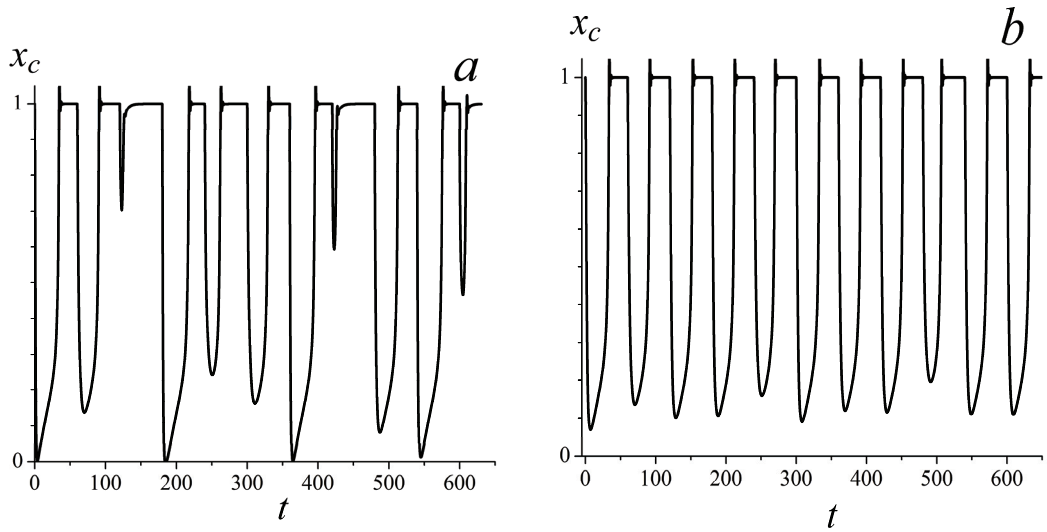

FIG. 4: The same as in Fig. 3, with application of the long pulse after the sequence of pulses shown in Fig. 2a and 2b. The duration of the long pulse is, $\tau \approx 2$.

dynamical chaos. Fig. 3 demonstrates the motion of the CT with the periodic repetition of the pulse sequences. (The period of repetition, $T = 60$, is much greater than the CT relaxation time $\tau_c = 1$.)

This irregular motion of the CT does not prevent the opportunity of the signal detection, as the cantilever each time deflects in the same direction. Our next goal was to find the possibility for quasi-periodic deflections of the cantilever in spite of the quasi-random dynamics. We have found that this could be realized by application of the additional long pulse (with duration $\tau = 2$ which is greater than the CT relaxation time, $\tau_c = 1$) after the pulse sequence shown in Fig. 2b. This long pulse causes a stabilization of the CT deflection. (See Fig. 4b.)

IV. CONCLUSION

We considered extension of the MRFM to the situation when a ferromagnetic probe is replaced with a paramagnetic one (PMRFM). We have found a sequence of *rf* pulses which causes a significant change of the magnetic force and the corresponding CT displacement from the equilibrium position. Repeated application of the pulse sequences will allow a detection of the quasi-random CT displacement. We have found the condition when the CT displacement becomes quasi-periodic which can significantly simplify its detection.

Finally, we note that MRFM has clear advantage in comparison with PMRFM. However PMFRM may substitute MRFM at temperatures above the Curie point where ferromagnetic particle cannot be used assuming that the temperature of a sample cannot be reduced.

References

[1] J.A. Sidles, J.L. Garleini, K.J. Bruland, D. Rugar, O.Zuger, S. Hoen, and C.S. Yannoi. Magnetic resonance force microscopy, Rev. Mod. Phys., **67**, 249-265 (1995).

[2]. G.P. Berman, F. Borgonovi, V.N. Gorshkov, and V.I. Tsifrinovich, *Magnetic Resonance Force Microscopy and a Single-Spin Measurement*, (World Scientific, 2006).

[3]. D. Rugar, R. Budakian, H. J. Mamin, and B. W. Chui, Single spin detection by magnetic resonance force microscopy, Nature*,* **430**, 329-332 (2004).

[4]. C.L. Degen, M. Poggio, H.J. Mamin, C.T. Rettner, and D. Rugar, Nanoscale magnetic resonance imaging, Proceedings of the National Academy of Sciences, **106(5)**, 1313(5) (2009).